A versatile water soluble fluorescent probe for ratiometric sensing of Hg^{2+} and bovine serum albumin

*Jinghan Wen, Zhirong Geng, Yuxin Yin, Zhilin Wang**

State Key Laboratory of Coordination Chemistry, Coordination Chemistry Institute, School of Chemistry and Chemical Engineering, Nanjing University, Nanjing 210093, P. R. China

**To whom correspondence should be addressed. E-mail: wangzl@nju.edu.cn.*

Content

1. ^{1}H NMR and ESI-MS Spectra of 1

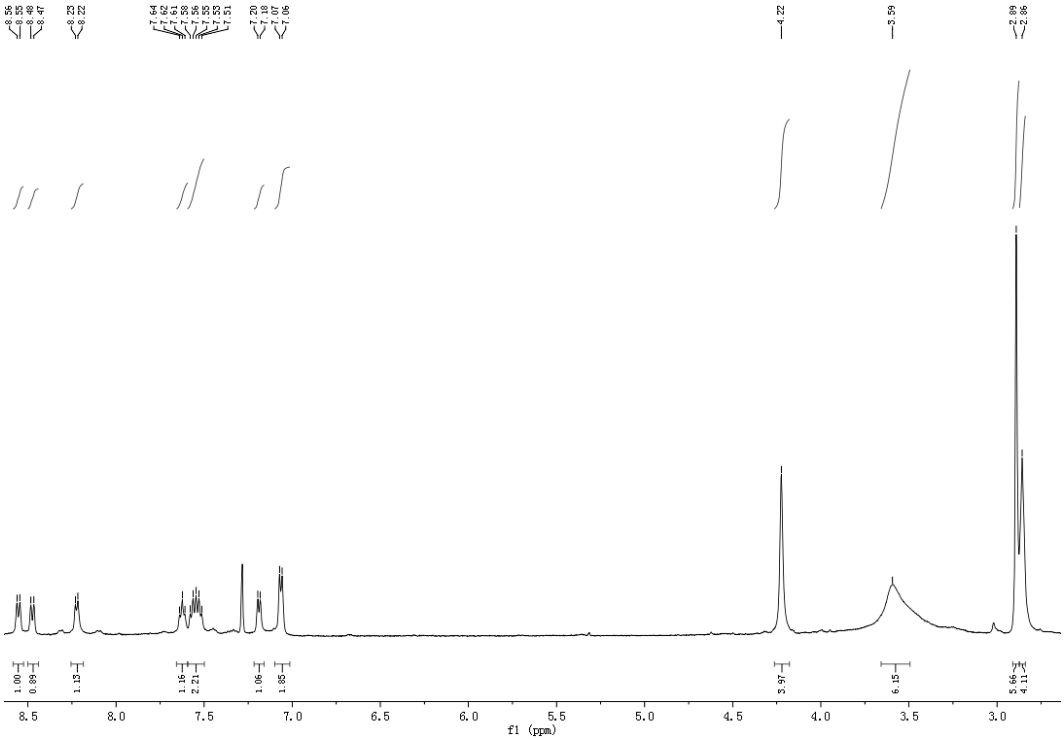

Fig. S1 ^{1}H NMR spectrum of **1** in $CDCl_3$ (500 MHz).

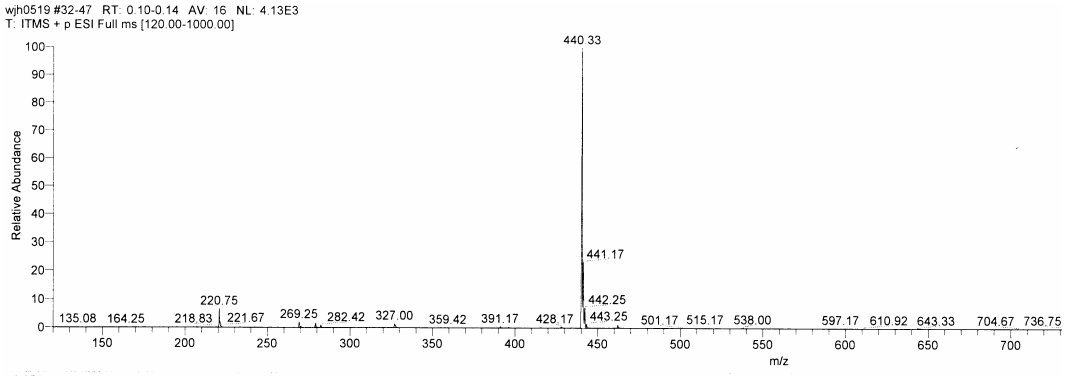

Fig. S2 ESI-MS spectrum of **1** in CH_3CN.

2. Hg^{2+} Fluorescent Response and Binding Behavior of 1

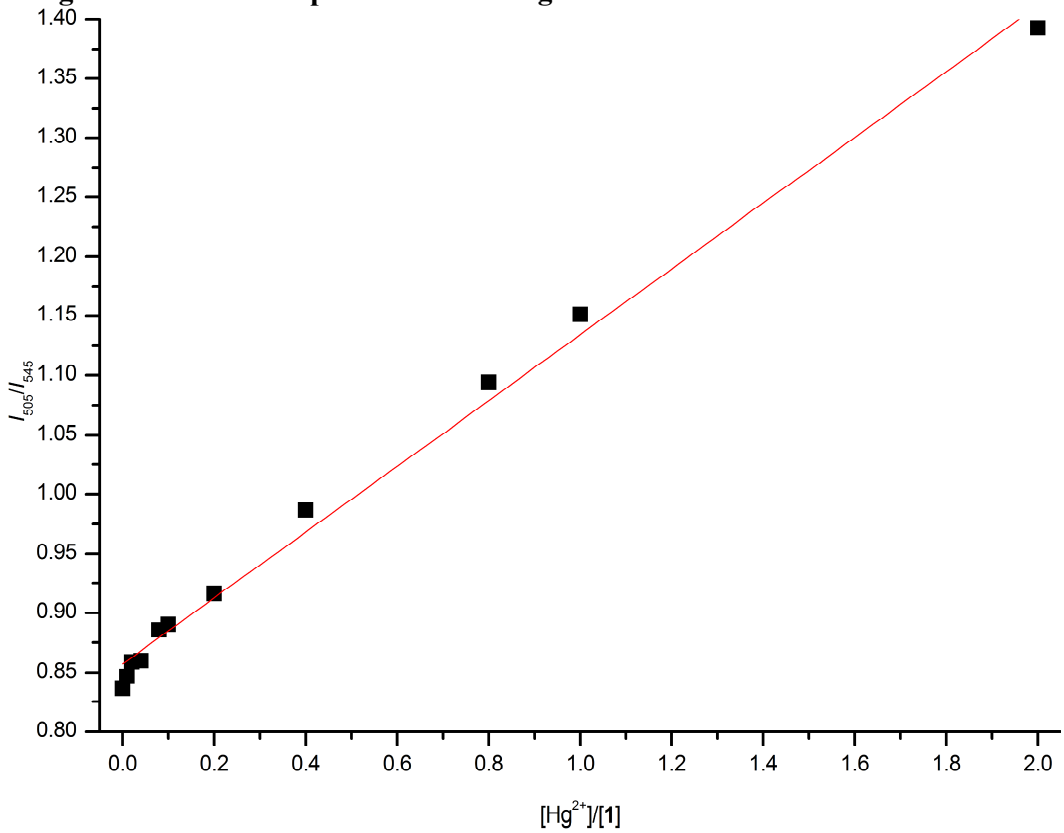

Fig. S3 The linear increasing range of the emission ratio (I_{505}/I_{545}) of 10 μM **1** vs. the concentration of Hg^{2+} in Tris-HCl buffer (50 mM, pH 7.6). λ_{ex}=330 nm.

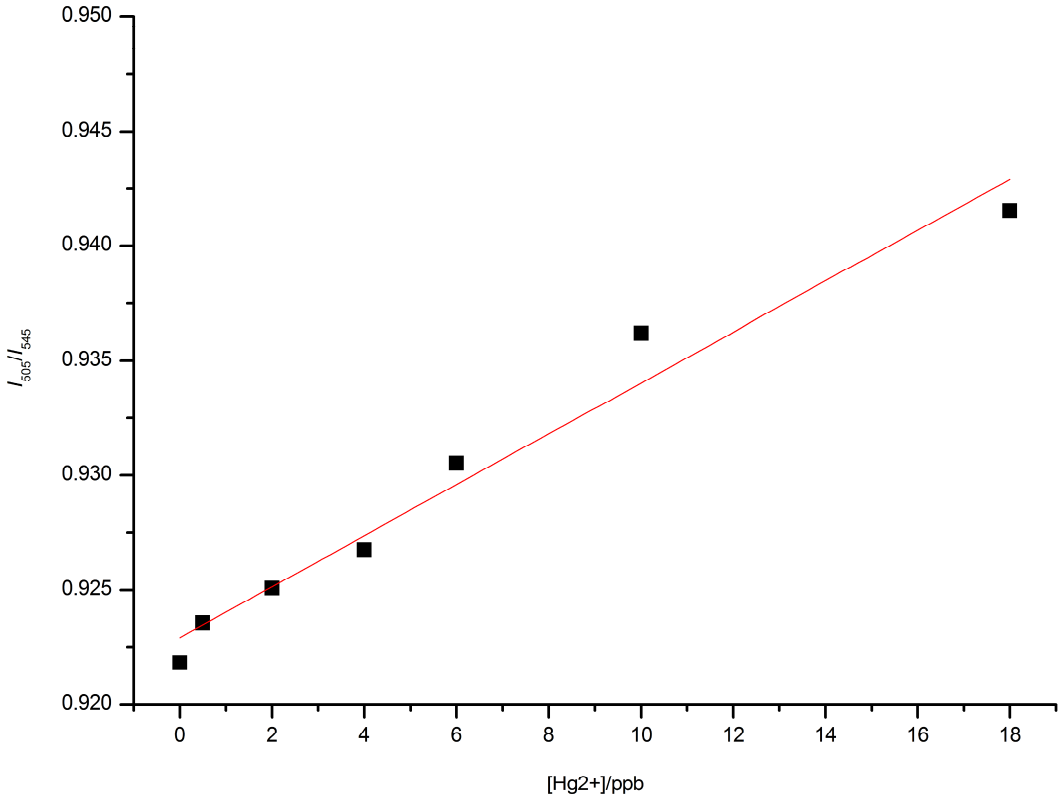

Fig. S4 The linear increasing of the emission ratio (I_{505}/I_{545}) of 5 μM **1** vs. the low concentration range of Hg^{2+} in Tris-HCl buffer (50 mM, pH 7.6). λ_{ex}=330 nm.

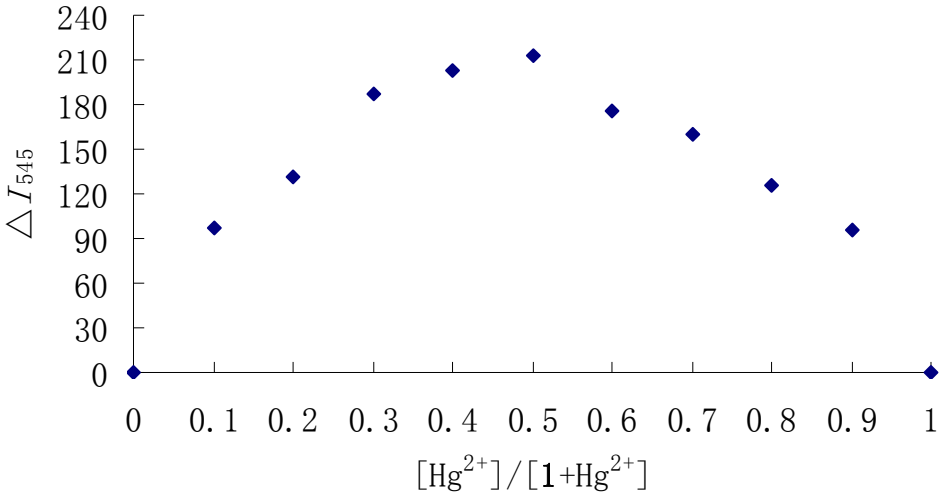

Fig. S5 Job's plot for the binding between **1** and Hg^{2+}. [**1**]+[Hg^{2+}]=20 μM. λ_{ex}=330 nm.

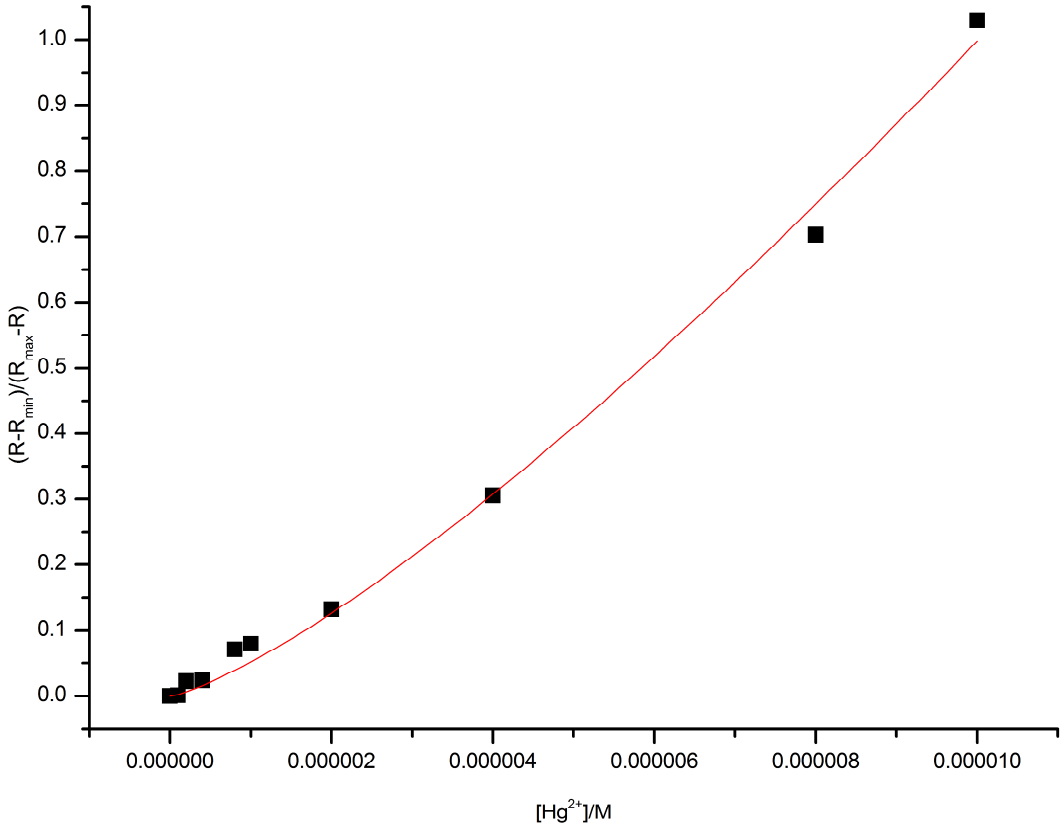

Fig. S6 The emission change of **1** induced by Hg^{2+} titration. The binding constant was obtained by nonlinear fitting to the data, and the red line is the resulted fitting line. R=I_{505}/I_{545}, λ_{ex}=330 nm.

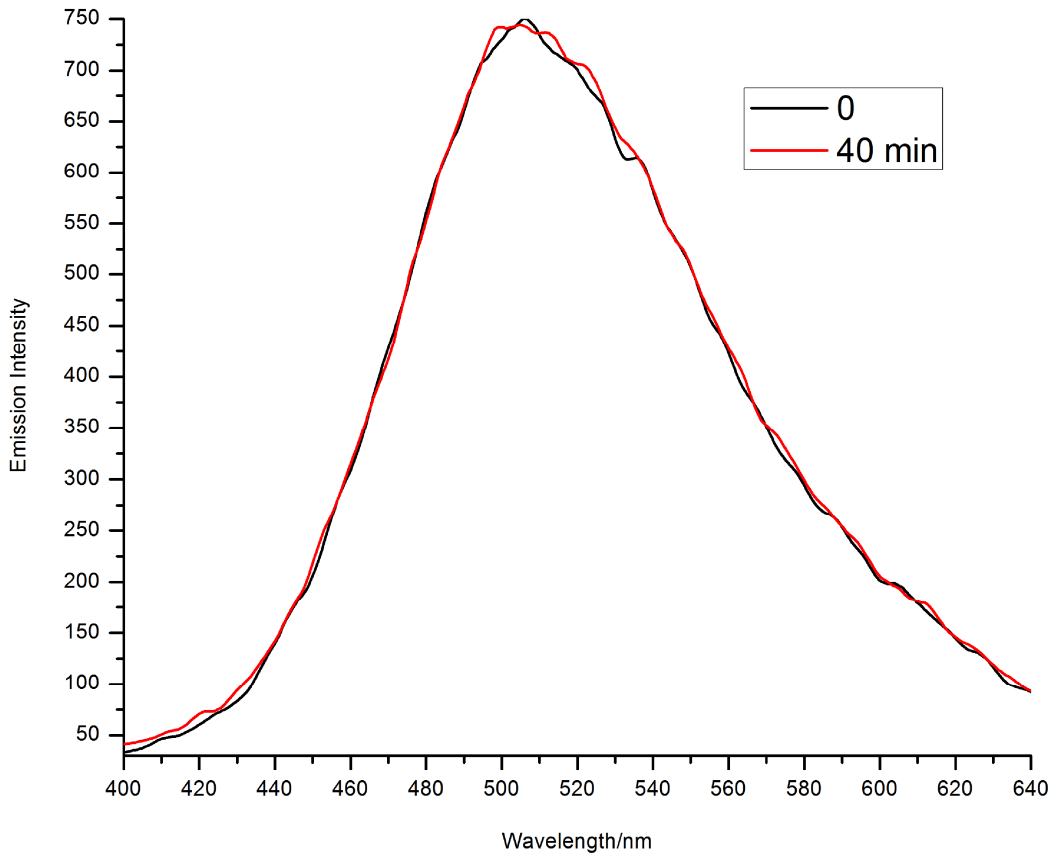

Fig. S7 Fluorescent spectra of 10 μM **1** in the presence of Hg^{2+} (5 equiv.) before and after UV irradiation at 330 nm for 40 min in Tris-HCl buffer (50 mM, pH 7.6).

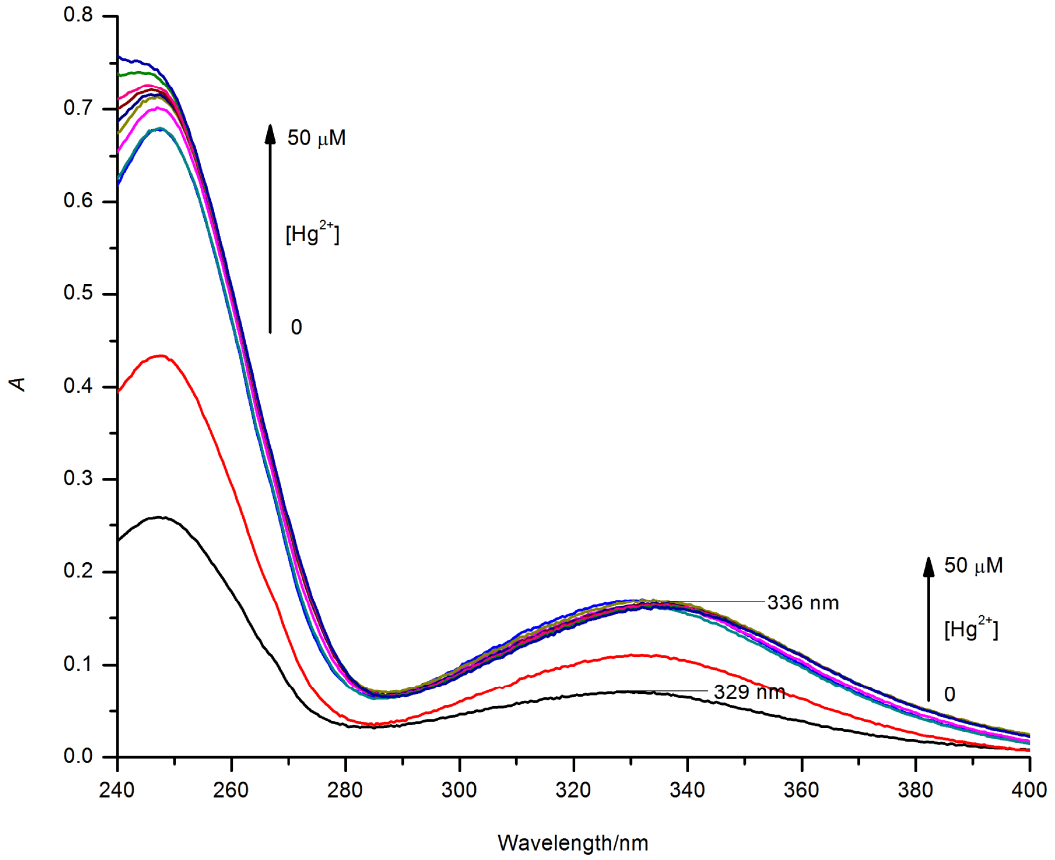

Fig. S8 UV-vis changes of 50 μM **1** upon addition of Hg^{2+} in Tris-HCl buffer (50 mM, pH 7.6).

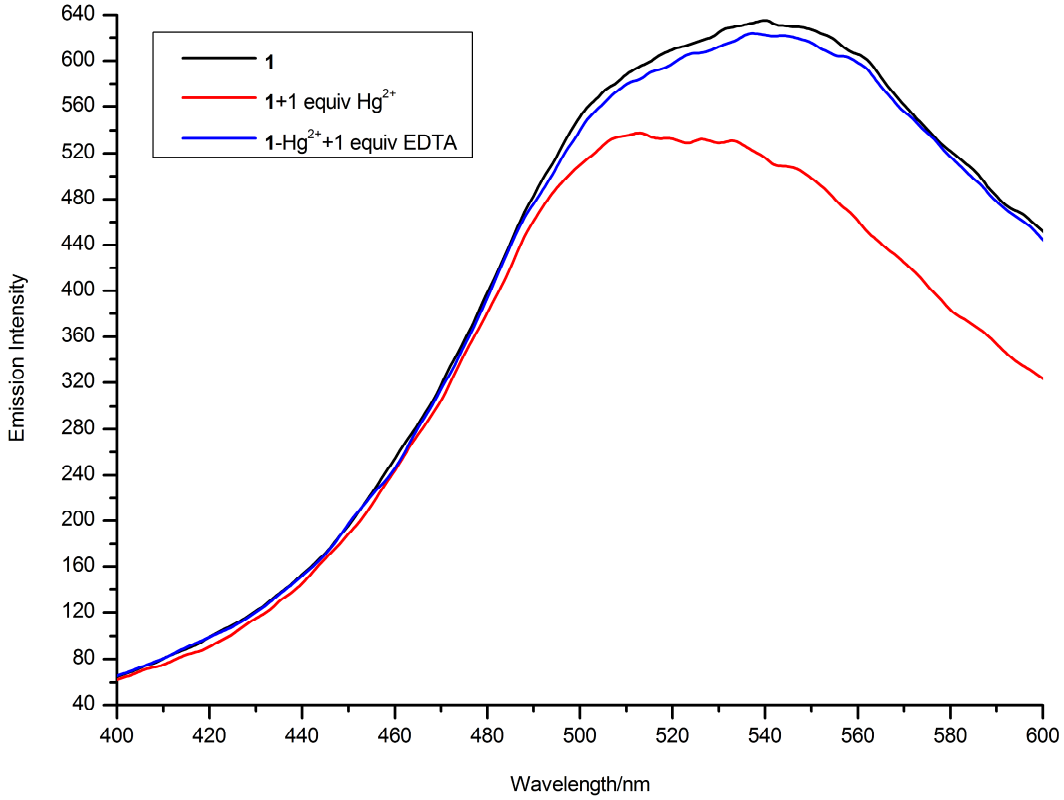

Fig. S9 Fluorescent changes of 10 μM **1** upon addition of 1 equiv. of Hg^{2+} and EDTA in Tris-HCl buffer (50 mM, pH 7.6). λ_{ex}=330 nm.

3. Fluorescent Response and Binding Pattern of 1 with BSA

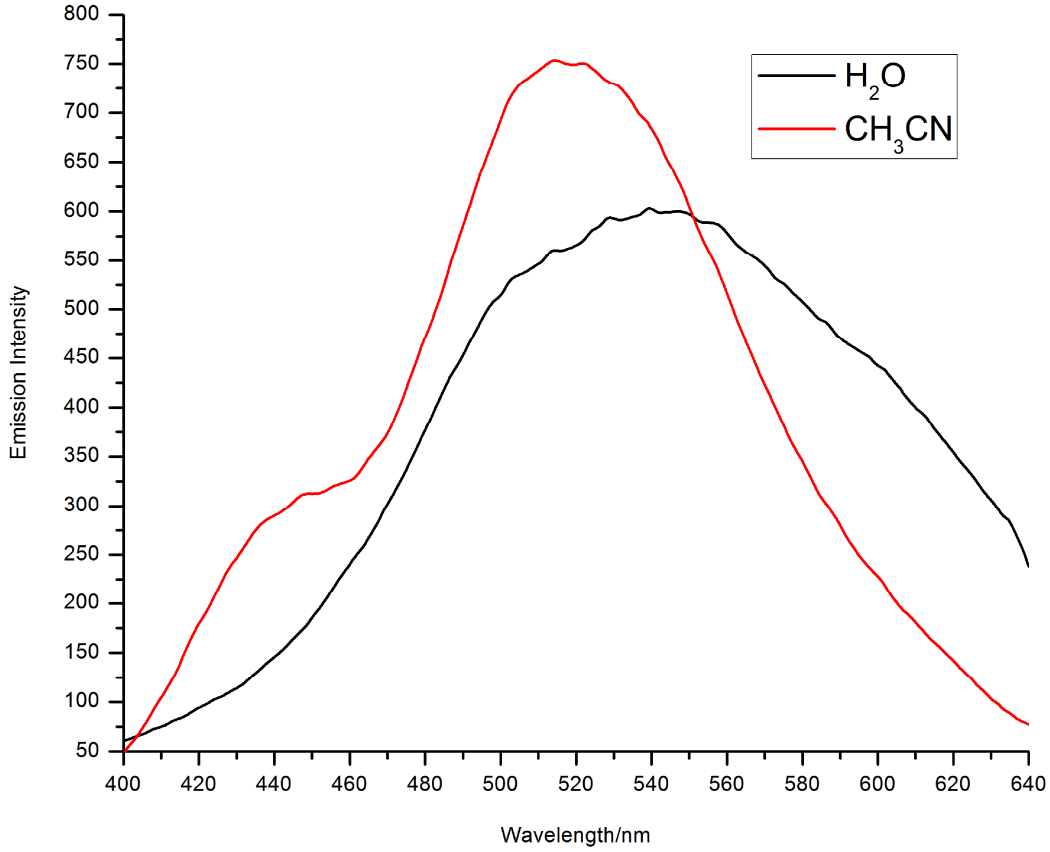

Fig. S10 Fluorescent spectra of 10 μM **1** Tris-HCl aqueous solution (50 mM, pH 7.6) and CH_3CN. λ_{ex}=330 nm.

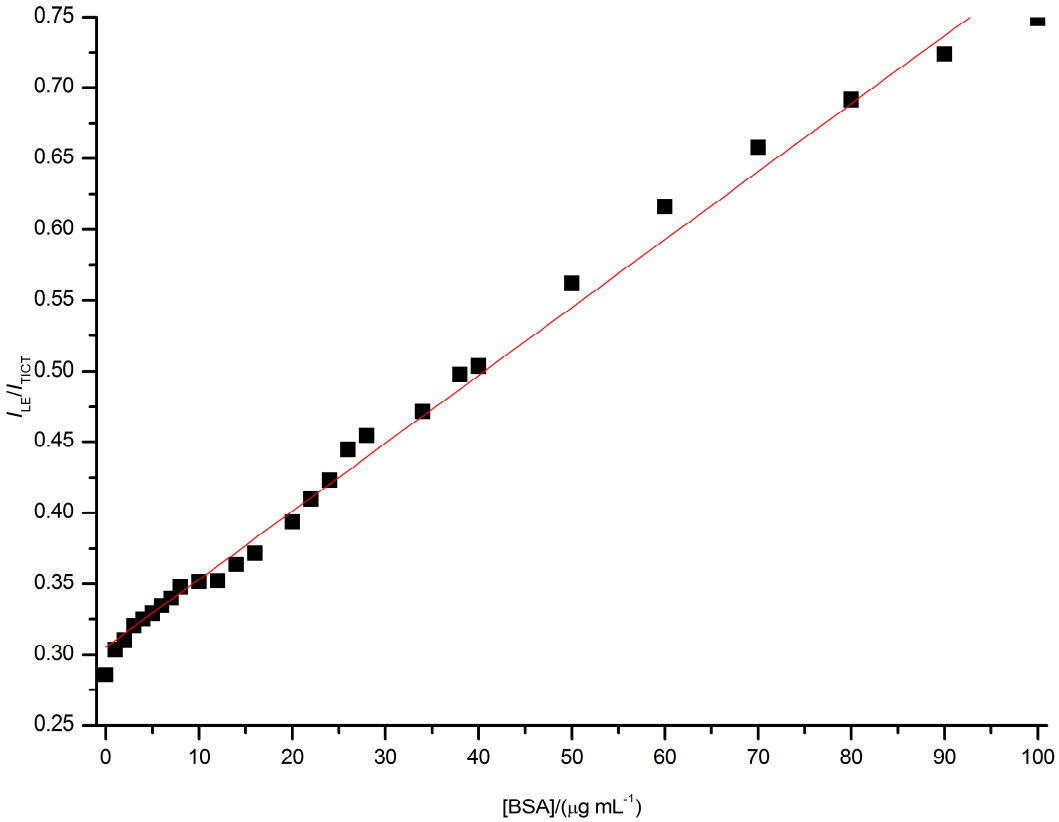

Fig. S11 The linear increasing range of the emission ratio (I_{LE}/I_{TICT}) of 10 μM **1** vs. the concentration of BSA in Tris-HCl buffer (50 mM, pH 7.6). λ_{ex}=330 nm.

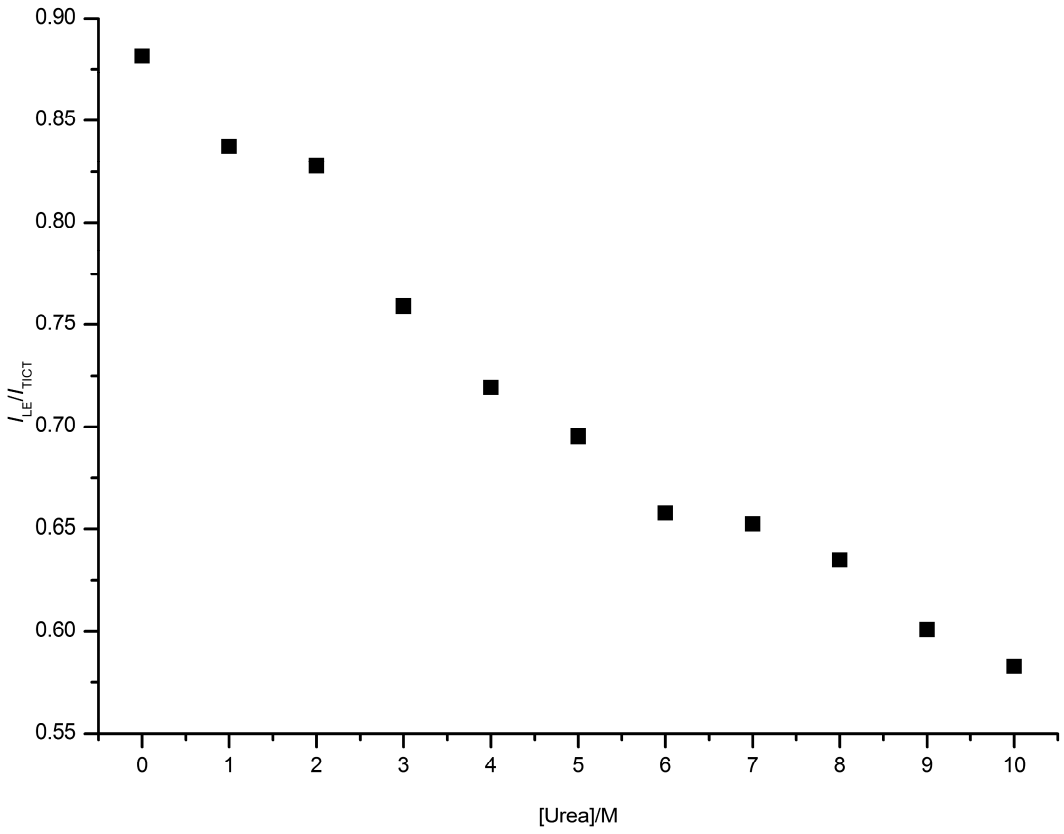

Fig. S12 The effect of different concentrations of urea on the fluorescent intensity of **1**-BSA in Tris-HCl buffer (50 mM, pH 7.6). λ_{ex}=330 nm.

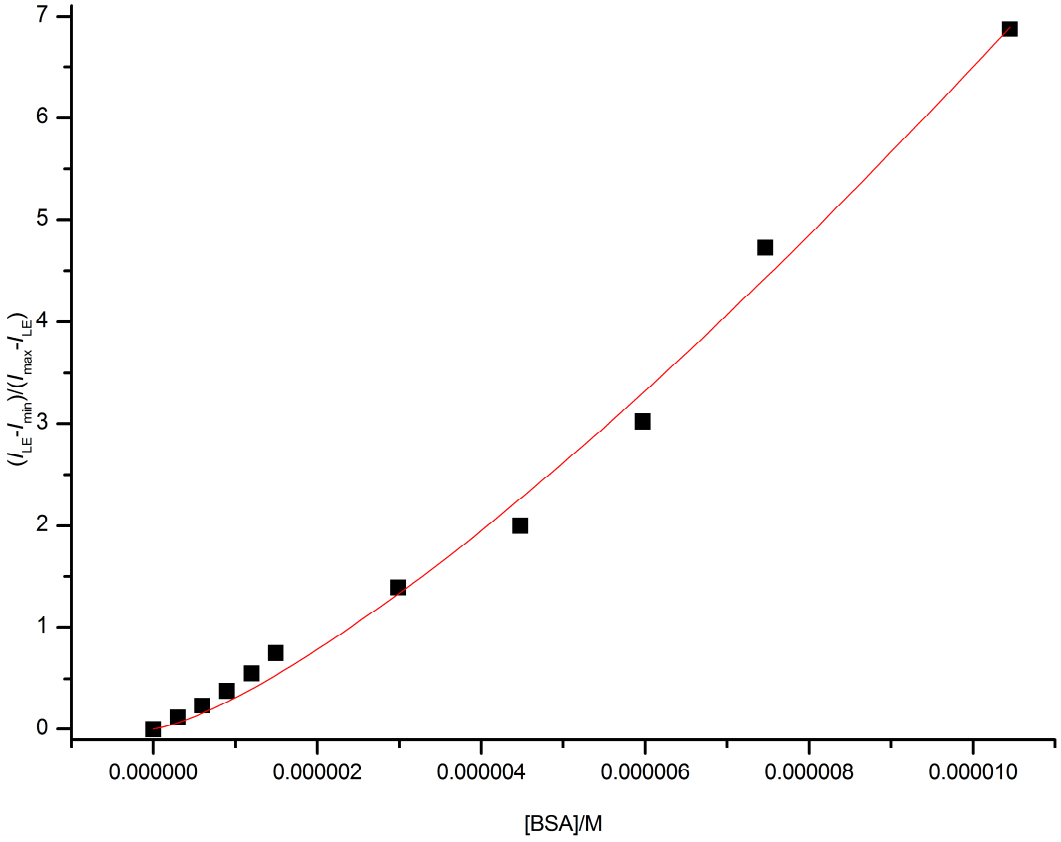

Fig. S13 The emission change of **1** induced by BSA titration. The binding constant was obtained by nonlinear fitting to the data, and the red line is the resulted fitting line. λ_{ex}=330 nm.

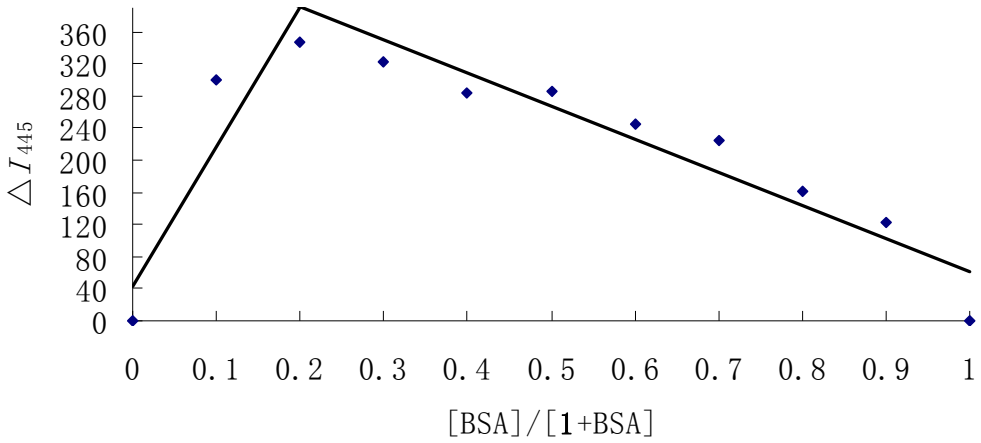

Fig. S14 Job's plot for the binding between **1** and BSA. [**1**]+[BSA]=20 μM. λ_{ex}=330 nm.

4. Computer Program for the Logic Gates Utilizing C Language

```
void Input_Output(int Input1, int Input2, int &Output_1, int &Output_2, int &Output_3)
{
   if (Input1>1 || Input1 <0 || Input2>1 || Input2<0 )
      printf("%s","Input error");
   else {
         Output_1 = Input2;
         Output_2 = Input1 | Input2;
         Output_3 = (!Input1) & (!Input2);
   }
}
```

5. **Computationally Optimized Energies and Coordinates of 1 and 1-Hg^{2+}**

(1) Energies of optimized compounds (a. u.):

1: -1706.9008428

1-Hg^{2+}: -1749.202072

(2) Coordinates of optimized compounds:

1:

Standard orientation:

Center Number	Atomic Number	Atomic Type	Coordinates (Angstroms) X	Y	Z
1	6	0	4.519706	2.356718	-1.746342
2	6	0	4.345976	1.063757	-1.244472
3	7	0	4.064926	0.851802	0.059037
4	6	0	3.875293	1.893049	0.893120
5	6	0	4.041029	3.211142	0.457634
6	6	0	4.380573	3.441075	-0.877335
7	6	0	4.390483	-0.183646	-2.126363
8	6	0	3.418231	1.549419	2.308751
9	7	0	3.096749	-0.852688	-2.368263
10	6	0	2.444677	-1.601931	-1.268612

11	6	0	1.437000	-0.739881	-0.457956
12	7	0	0.789534	-1.383385	0.717845
13	6	0	1.641083	-1.843796	1.859664
14	6	0	2.774342	-0.850318	2.183781
15	7	0	2.320977	0.552412	2.269635
16	6	0	-2.447478	-0.549115	0.257552
17	6	0	-3.352793	0.288422	-0.479934
18	6	0	-4.135913	1.269883	0.219821
19	6	0	-3.947424	1.428804	1.579477
20	6	0	-3.048414	0.603002	2.294936
21	6	0	-2.328949	-0.383562	1.664826
22	6	0	-1.710075	-1.499694	-0.487964
23	6	0	-1.846100	-1.666836	-1.839663
24	6	0	-2.711892	-0.812911	-2.558832
25	6	0	-3.431169	0.153704	-1.891130
26	16	0	-0.452578	-2.605808	0.306182
27	8	0	0.008214	-3.636774	-0.830244
28	8	0	-0.938055	-3.189966	1.711802
29	7	0	-5.078485	2.039374	-0.534000
30	6	0	-6.337054	1.316648	-0.868022
31	6	0	-5.339533	3.412480	-0.059653

32	1	0	4.754889	2.507944	-2.792955
33	1	0	3.891345	4.036069	1.143348
34	1	0	4.514424	4.453841	-1.239740
35	1	0	4.826054	0.077672	-3.097806
36	1	0	5.047073	-0.914621	-1.643302
37	1	0	3.042130	2.459672	2.785377
38	1	0	4.288232	1.200339	2.894476
39	1	0	2.445968	-0.284947	-2.914312
40	1	0	1.912790	-2.469829	-1.670942
41	1	0	3.237589	-1.965837	-0.609241
42	1	0	1.931562	0.132066	-0.036961
43	1	0	0.632082	-0.402463	-1.121805
44	1	0	2.116030	-2.816541	1.661173
45	1	0	0.971139	-1.975638	2.711709
46	1	0	3.258781	-1.212444	3.111917
47	1	0	3.517207	-0.866347	1.387151
48	1	0	1.627012	0.703081	3.004832
49	1	0	-4.524330	2.167763	2.121047
50	1	0	-2.959178	0.731875	3.367621
51	1	0	-1.707498	-1.072951	2.217729
52	1	0	-1.265314	-2.444796	-2.320845

53	1	0	-2.786321	-0.910294	-3.635085
54	1	0	-4.059581	0.854624	-2.424174
55	1	0	-6.096884	0.318249	-1.238357
56	1	0	-6.868051	1.869691	-1.649719
57	1	0	-6.997194	1.218601	0.009615
58	1	0	-4.388082	3.911651	0.139837
59	1	0	-5.962674	3.453508	0.850869
60	1	0	-5.864719	3.955832	-0.852307

1-Hg^{2+}:

Standard orientation:

Center Number	Atomic Number	Atomic Type	Coordinates (Angstroms) X	Y	Z
1	6	0	-5.337218	-2.160886	1.238411
2	6	0	-4.145569	-1.830096	0.596337
3	7	0	-4.034026	-0.617365	0.011617
4	6	0	-4.904366	0.393897	0.227631
5	6	0	-6.114901	0.115259	0.859530
6	6	0	-6.350876	-1.193197	1.307261

7	6	0	-2.814571	-2.610179	0.719848
8	6	0	-4.317025	1.807906	-0.002132
9	7	0	-1.817402	-1.572755	1.196546
10	6	0	-0.329472	-1.722241	1.209839
11	6	0	0.324784	-0.321396	1.504297
12	7	0	-0.141373	0.792258	0.587665
13	6	0	-0.541458	2.140828	1.156330
14	6	0	-1.846570	2.745141	0.524445
15	7	0	-2.949746	1.740979	0.650696
16	6	0	3.512942	0.456981	-0.105925
17	6	0	4.668354	-0.422474	-0.098457
18	6	0	5.857968	-0.033429	0.643279
19	6	0	5.755049	1.087563	1.479404
20	6	0	4.620341	1.902233	1.471694
21	6	0	3.521497	1.630974	0.669522
22	6	0	2.412523	0.003269	-0.890106
23	6	0	2.371828	-1.187747	-1.593696
24	6	0	3.467352	-2.051616	-1.489613
25	6	0	4.575865	-1.673254	-0.741533
26	16	0	0.906336	1.022244	-0.987826
27	8	0	-0.148645	0.243803	-2.013879

28	8	0	1.025519	2.597312	-1.159877
29	7	0	7.019386	-0.766203	0.550802
30	6	0	7.588822	-1.193478	-0.760540
31	6	0	8.039650	-0.660700	1.619243
32	1	0	-5.462226	-3.127898	1.708356
33	1	0	-6.838567	0.900243	1.037540
34	1	0	-7.290321	-1.433735	1.789596
35	1	0	-2.938281	-3.447277	1.414586
36	1	0	-2.478585	-3.002338	-0.247066
37	1	0	-4.975806	2.559995	0.443647
38	1	0	-4.190773	2.036646	-1.066480
39	1	0	-2.138438	-1.197976	2.097106
40	1	0	0.032051	-2.414886	1.981330
41	1	0	-0.001924	-2.099286	0.235774
42	1	0	0.074302	-0.014567	2.524795
43	1	0	1.413183	-0.430698	1.446326
44	1	0	0.259129	2.868889	0.989282
45	1	0	-0.675404	2.002681	2.233311
46	1	0	-2.055391	3.686869	1.048154
47	1	0	-1.672114	2.972225	-0.531465
48	1	0	-3.076727	1.496547	1.640381

49	1	0	6.603120	1.387316	2.077906
50	1	0	4.628942	2.806196	2.069572
51	1	0	2.721884	2.353362	0.580342
52	1	0	1.516891	-1.430846	-2.210085
53	1	0	3.445581	-3.008446	-1.994189
54	1	0	5.393738	-2.371049	-0.630102
55	1	0	6.903767	-0.944012	-1.570862
56	1	0	7.796438	-2.268187	-0.764647
57	1	0	8.529921	-0.655716	-0.929169
58	1	0	7.555043	-0.632149	2.597403
59	1	0	8.675305	0.226726	1.494808
60	1	0	8.672684	-1.550773	1.572920
61	80	0	-1.982142	-0.034140	-0.726194
